PHYSICAL REVIEW E VOLUME 59, NUMBER 6 JUNE 1999

Spatial multistability and nonvariational effects

M. Bachir, P. Borckmans, and G. Dewel
Service de Chimie-Physique and Center for Nonlinear Phenomena and Complex Systems, Code Postal 231, Université Libre de Bruxelles, 1050 Bruxelles, Belgium

(Received 22 February 1999)

We investigate the phenomenon of spatial multistability of fronts in thin bistable systems and stress the important role played by the absence of a variational principle. Nonvariational effects allow, for instance, two different immobilized fronts to coexist. The morphological instability of the corresponding nucleating solution can then lead, even in the absence of any diffusive instability, to nontrivial patterns in the depth of one-side-fed reactors. [S1063-651X(99)50406-6]

PACS number(s): 82.40.−g, 05.70.Ln, 47.54.tr

Multistability is a characteristic feature of many driven nonlinear systems. In a continuous stirred tank reactor (CSTR), autocatalytic reactions can, for instance, exhibit two stable homogeneous steady states for a range of values of the flow rate (bistability). On the other hand, the design of open spatial gel reactors has triggered a renewal in the experimental study of sustained spatial and spatiotemporal patterns in nonlinear chemical systems [1]. In this context, the one-side-fed reactor (OSFR) has proved very useful since it allows one to indefinitely maintain chemical waves [1,2] and Turing structures [3,4] at a controlled distance from equilibrium. It consists of a thin film of gel, one side of which is in contact with the content of a CSTR, while the opposite face is pressed against an impermeable solid surface. The patterns develop in the transverse direction parallel to the plates and they are observed in the longitudinal direction, orthogonal to the film. If the gel is thin enough, the concentrations are expected to be almost constant through its depth and the patterns can be considered to a good approximation as two-dimensional. However, it has been pointed out recently that in the case of bistable systems, concentration profiles can develop along the longitudinal direction. These immobilized fronts, which can coexist with one of the trivial homogeneous steady states (spatial bistability), must be taken into account in the interpretation of the experiments performed in a OSFR [5].

In this Rapid Communication, we investigate this phenomenon of spatial multistability on simple models by stressing the crucial role played by the nonvariational effects. For instance, the absence of a variational principle allows two different immobilized fronts to exist for the same values of the constraints and boundary conditions (BC). The physical meaning of these concepts can be clarified by considering as an illustration the following two-variable reaction-diffusion model:

$$\epsilon u_t = f(u) - v + \epsilon^2 \nabla^2 u, \tag{1}$$

$$v_t = \gamma u - v - b + \nabla^2 v, \tag{2}$$

where ϵ and b are positive constants and γ plays the role of the bifurcation parameter. To be able to compare analytical results with numerical simulations, we first set

$$f(u) = -u + H(u-a), \quad b = 5a, \tag{3}$$

[$H(x)$ is the Heaviside step function] recovering a variant of the piecewise linear McKean model [6]. Such a model has been used in the study of localized patterns consisting of a droplet of one state embedded in another state [7,8].

For $\gamma_l < \gamma < \gamma_h$ [where $\gamma_l = 4$ and $\gamma_h = (4a+1)/a$] the system admits two stable homogeneous steady states: a lower branch $u_l = 5a/(\gamma+1)$; $v_l = -u_l$ and an upper branch $u_h = (5a+1)/(\gamma+1)$; $v_h = (\gamma - 5a)/(\gamma+1)$ of solutions. Concentration fronts connecting these two states can also be formed. When ϵ is small, u undergoes an abrupt change in this wave (''propagator'' species), whereas the level of v in the front controls its speed and direction (''controller'' species). In unbounded variational systems, such fronts propagate without deformation in such a way as to increase the territory of the most stable (dominant) state and finally restore uniformity. Incompatible BC or nonvariational effects can immobilize these fronts and give rise to asymmetric steady solutions [9]. Such nonuniform stationary states also play an important role, for instance, in the Couette flow reactor [10,11], heterogeneous catalytic systems [9,12], the ballast resistor [13], and resistive domains in superconductors [14]. In a OSFR asymmetric BC occur naturally. Along the surface in contact with the CSTR ($x=0$), the concentrations take values corresponding to one of the homogeneous steady states. Let us consider

$$u = u_h, \quad v = v_h, \quad \text{at} \quad x = 0. \tag{4}$$

No flux BC are required on the other side,

$$\frac{\partial u}{\partial x} = \frac{\partial v}{\partial x} = 0 \quad \text{at} \quad x = L. \tag{5}$$

In such a configuration, concentrations corresponding roughly to the other steady state (here u_l, v_l) can be attained along the solid surface at $x=L$. Because we are mainly interested in the formation of concentration profiles inside the gel, we start by studying the one-dimensional version of our problem.

For the sake of comparison, we first consider the case of the variational model that can be obtained by substituting the value $v=\gamma u-b$ in Eq. (1). The corresponding evolution equation then takes the form

$$\epsilon u_t=-(\gamma+1)u+5a+H(u-a)+\epsilon^2\frac{\partial^2 u}{\partial x^2} \tag{6}$$

$$=-\frac{\delta V}{\delta u}+\epsilon^2\frac{\partial^2 u}{\partial x^2}. \tag{7}$$

The solutions u_l and u_h correspond to minima of the potential,

$$V=\left(\frac{\gamma+1}{2}\right)u^2-5au-\int_0^u du' H(u'-a). \tag{8}$$

The parameter value $\gamma_M=(8a+1)/2a$ defines the Maxwell point at which $V(u_l)=V(u_h)$. When $\gamma>\gamma_M$, u_l is the most stable state and u_h is metastable. This situation is reversed when $\gamma<\gamma_M$.

Besides the trivial solution $u=u_h$, with the BC defined above, the system admits an inhomogeneous steady state corresponding to an immobilized front. In a semi-infinite system, it separates the upper branch at $x=0$ from the other steady state u_l at $x=\infty$. The immobility condition for this kink then takes the form

$$\frac{\epsilon^2}{2}\left(\left.\frac{\partial u}{\partial x}\right|_0\right)^2=V(u_h)-V(u_l). \tag{9}$$

Such a solution thus only exists when the state, fixed at the $x=0$ boundary, is a metastable state [i.e., when $V(u_h)>V(u_l)$, $\gamma>\gamma_M$].

In finite systems, the concentration at the solid surface now attains in the profile a value u_L that is higher than that of the lower branch. The position σ of the front, which can be deduced from the condition $u(\sigma)=a$, is given by

$$\frac{\cosh[\alpha(L-2\sigma)]}{\cosh[\alpha L]}=2a(\gamma-\gamma_M), \tag{10}$$

where $\alpha^2=(\gamma+1)/\epsilon^2$.

This equation admits two solutions for σ, the smallest corresponding to a stable profile. At $\gamma=\gamma_c>\gamma_M$, these solutions annihilate and only the trivial state $u=u_h$ remains for $\gamma<\gamma_c$. γ_c is determined by substituting $\sigma_c=L/2$ into Eq. (12).

A similar analysis can be applied to the complementary case where the concentration imposed at $x=0$ is equal to u_l. A boundary layer in the form of a hole near the origin then occurs for $\gamma<\gamma_c'<\gamma_M$. For each value of γ in the bistable region, there is thus a minimum length below which no stable front exists (Fig. 1).

These asymmetric steady states occur as the result of a combination of bulk kinetics, favoring the most stable state of the bistable and a fixed BC imposing the metastable state. The front between these two states transforms itself into a boundary layer on approaching the surface where the concentration has been fixed. The same conclusions are valid for

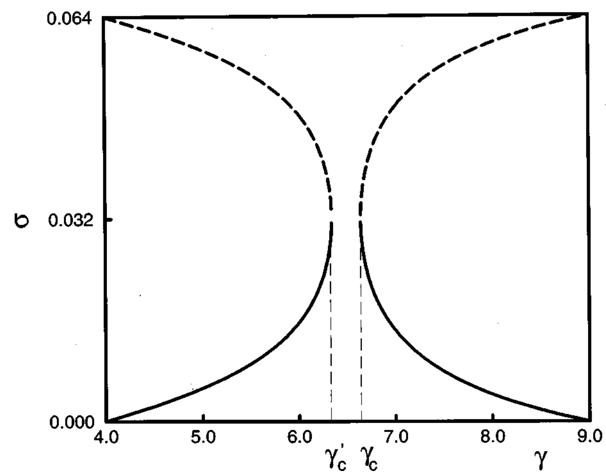

FIG. 1. Width σ of the boundary layer vs γ in the variational case [Eq. (8)]. $a=0.2$, $\epsilon=0.05$, and system length: $L=0.064$ (all constants are in arbitrary units). The solutions appearing in the range $4<\gamma<\gamma_c'$ correspond to the BC: $u=u_l$ at $x=0$; those occurring for $\gamma_c<\gamma<\gamma_h$ develop when $u=u_h$ at $x=0$. Solid and dashed lines denote stable and unstable solutions, respectively.

any gradient system that can be described by an evolution equation similar to Eq. (9). In a range of values of the bifurcation parameter excluding a region centered on the Maxwell point, finite variational systems thus exhibit a trivial case of spatial bistability between the homogeneous metastable steady state and a boundary layer that develops when this state is fixed at one boundary.

The situation is very different in the case of nonvariational systems, such as the model described by Eqs. (1) and (2). The inhomogeneous steady solutions that can develop in the presence of the asymmetric BC defined above now take the form $(i,j=1,2)$

$$u_s(x)=\sum_{i,j\neq i}A_{ij}\frac{\sinh[\alpha_j(L-\sigma)]}{\cosh[\alpha_j L]}\sinh[\alpha_j x]+u_h,\quad x<\sigma, \tag{11}$$

$$=-\sum_{i,j\neq i}A_{ij}\frac{\cosh[\alpha_j\sigma]}{\cosh[\alpha_j L]}\cosh[\alpha_j(L-x)]+u_l,\quad x>\sigma, \tag{12}$$

and

$$v_s(x)=\left(\epsilon^2\frac{d^2}{dx^2}-1\right)u_s(x)+H(\sigma-x). \tag{13}$$

The α are the zeros of the polynomial

$$\epsilon^2\alpha^4-\alpha^2(\epsilon^2+1)+(\gamma+1)=0. \tag{14}$$

With the parameter values considered in our simulations, Eq. (14) admits two positive and two negative roots $(\pm\alpha_1;\pm\alpha_2)$. The coefficients A_{ij} are determined by the BC and the matchings of $u_s(x)$, $v_s(x)$ and their derivatives at $x=\sigma$. We get

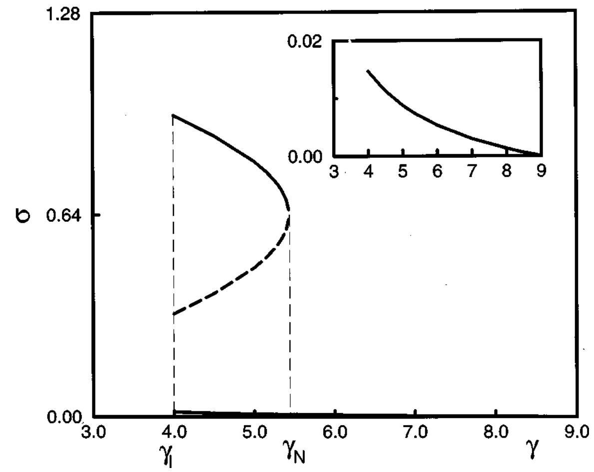

FIG. 2. Position σ of the immobilized fronts in the nonvariational case [Eqs. (1)–(3)]; $a=0.2$, $\epsilon=0.05$, and system length $L=1.28$ (all constants in arbitrary units), when $u(0)=u_h$. In the inset, the variation of the narrow boundary layer σ_1 is represented by γ. In the region of multistability ($\gamma_l=4<\gamma<\gamma_N$) the larger value σ_3 gives the position of the stable immobilized kink. The nucleating solution for the transition between these stable fronts is denoted by dashed line (σ_2).

$$A_{ij}=\frac{1+\epsilon^2\alpha_i^2[u_l-u_h]}{\epsilon^2(\alpha_i^2-\alpha_j^2)}. \qquad (15)$$

The position of the immobilized fronts is determined by the condition $u(\sigma)=a$. Using Eq. (13) or Eq. (14), this relation yields a transcendental equation for σ. It admits a stable solution corresponding to a narrow boundary layer ($\sigma_1\approx\epsilon$) in the entire region of bistability ($\gamma_l<\gamma<\gamma_h$). Moreover, two new solutions ($\sigma_2<\sigma_3$) appear at $\gamma=\gamma_N$. The larger value σ_3 gives the position of a stable immobilized kink (Fig. 2). For $\gamma<\gamma_N$, this system therefore exhibits spatial tristability between two immobilized fronts and the homogeneous steady state (u_h). The unstable profile (σ_2) provides the nucleating solution for the transition between the two immobilized fronts. Numerical integrations of Eqs. (1) and (2) with Eq. (3) produce profiles that coincide with the analytical expressions given above. Note that the large boundary layer (σ_3) appears in the range $\gamma<\gamma_M$, where the state u_h is dominant [$V(u_h)<V(u_l)$]. In the corresponding variational model, the BC defined by Eqs. (6) and (7) only lead in this range to transient propagating fronts that finally generate the uniform state u_h. Here such a front can be immobilized at a position where the controller species v attains a value corresponding to the Maxwell condition (i.e., $v_M=\frac{1}{2}-a\approx0.3$). This multiplicity of inhomogeneous solutions presents strong similarities to the nonequilibrium Ising-Bloch transition [15,16], which gives rise in unbounded nonvariational systems to the occurrence of two different fronts propagating in opposite directions for the same values of the constraints.

The interplay between these steady asymmetric solutions can generate nontrivial spatial patterns in two-dimensional systems that correspond to a longitudinal section of the gel. The planar nucleating solution (σ_2) is also unstable with respect to transverse modulations along the y direction [17]. In the perturbed front, the curvature induces an accumulation of the highly diffusive controller species in the concave regions [B in Fig. 3(a)], and a depletion in the convex segments [A in Fig. 3(a)]. On the other hand, the position of this front is determined by the local value v_f of the controller species in the transition region. The width of the activated domain ($u>a$) decreases when v_f increases. As a result the concave regions recede and fall onto the narrow boundary layer (σ_1), while the convex segments advance towards σ_3. As shown in Fig. 3 the initial modulation is then amplified. Finally this morphological instability gives rise to a periodic row of spots adjacent to a narrow switching front between the upper and lower branch. Note, however, that our model exhibits no Turing instability on the stable branches u_l and u_h.

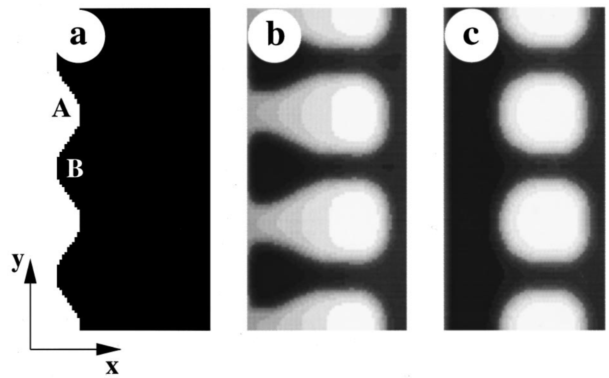

FIG. 3. Development of the morphological instability of the nucleating solution obtained by a two-dimensional numerical integration of the piecewise nonvariational model. $a=0.2$, $\epsilon=0.05$, $\gamma=4.01$, and system lengths $Lx=1.28$ and $Ly=2.56$ (all constants in arbitrary units). (a) Initial transverse perturbation of the nucleating solution. (b) Convex segments advance while concave ones recede. (c) Final asymptotic periodic pattern.

The properties we have discussed are not specific to the piecewise linear character of the model. Indeed we have obtained similar results by integrating Eqs. (1) and (2) with the cubic nonlinearity

$$f(u)=u(u-a)(1-u). \qquad (16)$$

In conclusion, we have shown that the synergy between spatial multistability of fronts and the morphological instability of the corresponding nucleating solution can lead to nontrivial patterns in the depth of a OSFR, even in the absence of diffusive instabilities, as was also the case in experiments with the ferrocyanide-iodate-sulfite system [18].

We thank J. Boissonade, P. De Kepper, and S. Métens for stimulating discussions. P.B. and G.D. received support from the FNRS (Belgium) and M.B. received support from the ''Direction de l'Enseignement Supérieur'' (Morocco) and the ''Fondation Universitaire D. and A. Van Buuren'' (Belgium).

[1] W.Y. Tam, W. Horsthemke, Z. Noszticzius, and H.L. Swinney, J. Chem. Phys. **88**, 3395 (1991).
[2] C.S. Skinner and H.L. Swinney, Physica D **48**, 1 (1991).
[3] R.D. Vigil, Q. Ouyang, and H.L. Swinney, Physica A **188**, 17 (1992).
[4] B. Rudovics, Ph.D. thesis, Universite de Bordeaux, 1995 (unpublished).
[5] P. Blanchedeau and J. Boissonade, Phys. Rev. Lett. **81**, 5007 (1998).
[6] H.P. McKean, Adv. Math. **4**, 209 (1979).
[7] S. Koga and Y. Kuramoto, Prog. Theor. Phys. **63**, 106 (1980).
[8] T. Otha, M. Mimura, and R. Kobayachi, Physica D **34**, 115 (1989).
[9] L.M. Pismen, Chem. Eng. Sci. **34**, 563 (1979).
[10] Q. Ouyang *et al.*, J. Chem. Phys. **95**, 351 (1991).
[11] A. Arneodo and J. Elezgaray, Phys. Lett. A **143**, 25 (1990).
[12] D. Luss and M.A. Ervin, Chem. Eng. Sci. **27**, 315 (1972).
[13] D. Bedeaux, P. Mazur, and R.A. Pasmanter, Physica A **86**, 355 (1977).
[14] R.C. Mints and A.V. Gurevich, Rev. Mod. Phys. **59**, 941 (1987).
[15] P. Coullet *et al.*, Phys. Rev. Lett. **65**, 1352 (1990).
[16] A. Hagberg and E. Meron, Phys. Rev. E **48**, 705 (1993).
[17] Y. Kuramoto, *Chemical Oscillations, Waves, and Turbulence* (Springer-Verlag, Berlin, 1984).
[18] K.J. Lee, W.D. McCormick, Q. Ouyang, and H.L. Swinney, Science **261**, 192 (1993).